Low-dose dose-response for reduced cell viability after exposure of human keratinocyte (HEK001) cells to arsenite

Kenneth T. Bogen [a],[*], Lora L. Arnold [b], Aparajita Chowdhury [d],[1], Karen L. Pennington [b], Samuel M. Cohen [b],[c]

[a] Health Sciences, Oakland, CA, USA
[b] Department of Pathology and Microbiology, University of Nebraska Medical Center, Omaha, NE, USA
[c] Havlik-Wall Professor of Oncology
[d] University of Nebraska Medical Center, USA

ABSTRACT

The in vitro arsenite (As[III]) cytotoxicity dose-response (DR) of human keratinocytes (HEK001) was examined at greater statistical resolution than ever previously reported using the MTT assay to determine cell viability. Fifty-four 96-well plates were treated with As[III] concentrations of 0.25, 0.5, 1, 2, 3, 4, 5, 7, 10, 15, 20, 25, or 30 μM. Because of unexpected variation in viability response patterns, a two-stage DR analysis was used in which data on plate-specific viability (%), estimated as 100% times the ratio of measured viability in exposed to unexposed cells, were fit initially to a generalized lognormal response function positing that HEK001 cells studied consisted of: a proportion P of relatively highly sensitive (HS) cells, a proportion P_o of relatively resistant cells, and a remaining $(1-P-P_o)$ fraction of typical-sensitivity (TS) cells exhibiting the intermediate level of As[III] sensitivity characteristic of most cells in each assay. The estimated fractions P and P_o were used to adjust data from all 54 plates (and from the 28 plates yielding the best fits) to reflect the condition that $P=P_o=0$ to provide detailed DR analysis specifically for TS cells. Four DR models fit to the combined adjusted data were each very predictive ($R^2 > 0.97$) overall but were inconsistent with at least one of the data set examined ($p < 10^{-5}$). Adjusted mean responses at $\leq 3\,\mu$M were approximately equal ($p > 0.30$) and exceeded 100% significance ($p \leq 10^{-6}$). A low-dose hormetic model provided the best fit to the combined adjusted data for TS cells ($R^2 = 0.995$). Marked variability in estimates of P (the proportion of apparent HS cells) was unexpected, not readily explained, and warrants further study using additional cell lines and assay methods, and in vivo.

© 2016 Published by Elsevier Ireland Ltd. This is an open access article under the CC BY-NC-ND license (http://creativecommons.org/licenses/by-nc-nd/4.0/).

1. Introduction

Inorganic arsenic (iAs) at high doses is a known human carcinogen to urinary bladder, lung and skin [1]. In addition to carcinogenic effects, recent data suggest that chronic high exposure to iAs may also contribute to other non-carcinogenic health effects such as cardiovascular diseases, obesity, diabetes, developmental defects, and respiratory diseases [2–4].

iAs has been proposed as a threshold carcinogen for at least two decades [5–8]. However, methods used have been inadequate to address this in a statistically rigorous fashion [7], although data from epidemiology studies, in animals, and in vitro as well as mechanistic research clearly support the likelihood that iAs toxicity has a threshold dose below which health effects are not expected [8]. Although the threshold question for iAs remains highly controversial [9,10], recent evidence supports the possibility of a threshold for iAs-induced cancer and toxic effects, including in vitro studies [11–13], animal studies [14,15], and epidemiologic investigations [16–20]. Strikingly consistent no-effect levels have been reported in animal models (approximately 1 ppm in water or diet) [8] and in vitro (>0.1 μM trivalent arsenicals) [8,11,12]. A general lack of increased (e.g., bladder) cancer risk in human populations exposed to arsenic in drinking water at concentrations below 100–150 ppb [8,16,19,20] is consistent with the associated non-cytotoxic internal concentrations of trivalent arsenic metabolites (e.g., <0.1 μM) in urine. Recent evidence is also consistent with thresholds for non-cancer endpoints of iAs exposure [8,15,17,18]. A practical threshold for cancer induced by exposure to iAs is thus possible in view

* Corresponding author at: Health Sciences 475 14th Street, Suite 400 Oakland, CA 94612, USA.
E-mail address: kbogen@exponent.com (K.T. Bogen).
[1] Current address: 2310 Commonwealth Avenue, Newton, MA 02466, USA.

of evidence that regenerative cell proliferation associated only with cytotoxic levels of iAs exposure consistently precedes iAs-exposure-induced epithelial tumors, such as urinary bladder, skin, and lung carcinomas [8,12,13]. Chemically induced regenerative cell proliferation, in turn, is a response to induced cell killing that for many chemicals is expected to have a threshold-like, S-shaped dose-response [21], as is the case for a wide array of metals (including iAs) and oxidative chemicals that stimulate the cytoprotective Nrf2-mediated antioxidant response element (ARE) pathway that generally is cytoprotective at relatively low levels of increased expression [22–24].

Low-dose nonlinearity for arsenic-induced cytotoxicity in vitro is suggested by data reported in previous studies done using various cell lines [13,21,25–27]. However, relatively small replicate numbers used in such studies limited their statistical power to resolve details of cytotoxic dose-response observed low concentrations, including those associated with relatively small departures from background response levels. The present study aimed to develop more detailed data adequate to assess whether the low-dose dose-response pattern exhibited by reductions in cell viability in vitro following exposure to trivalent arsenic is consistent with a linear or nonlinear (e.g., threshold-like) pattern. This study used more than 50 assay replicates conducted at 14 iAs concentrations specially selected to focus specifically on the initial portion of the low-dose dose-response curve for reduced cell viability. For reasons of practical feasibility in a first study conducted at this level of detail, a key limitation of the study design was that concentration effects were investigated using only a single cell line and single (MTT) assay method, with the recognition that broader generalizations concerning observed response patterns can only be based on results of similarly detailed studies using additional cell types and cytotoxicity assay methods.

2. Methods

2.1. Materials

Sodium arsenite (NaAsO$_2$) (NaAs^{III}) (99% purity as certified by the vendor) purchased from Sigma (St. Louis, MO) was used without additional analysis. A 10 mM stock solution was prepared in Dulbecco's PBS 1X (Gibco, Grand Island, NY). Treatment solutions of As^{III} at concentrations (C_i) of 0.25, 0.5, 1, 2, 3, 4, 5, 7, 10, 15, 20, 25, and 30 μM, were prepared in cell culture medium fresh on the day of treatment. Levels of iAs, monomethylarsonic acid (MMA) and dimethylarsinic acid (DMA) were determined for Dulbecco's PBS 1X and cell culture medium using hydride generation-atomic absorption spectrometry coupled with cryotrap (HG-CT-AAS). For Dulbecco's PBS 1X, the concentration of iAs was 0.187 ng/mL, and concentrations of MMA and DMA were below the detection limit (0.05 ng arsenic/mL for both). In the cell culture medium, concentrations were below the detection limit for iAs (0.1 ng arsenic/mL), MMA and DMA. The 13 test concentrations were selected, based on preliminary experiments and analysis of data from a previous study of As^{III}-induced cytotoxicity in HEK001 cells [13], to yield a relatively detailed expected characterization of dose-response for As^{III}-induced cytotoxicity, including at relatively low levels of this response in the range of 85% to 100% viability relative to unexposed cells.

2.2. Cell culture

The HEK001 human keratinocyte cell line, derived from normal human skin and immortalized by transfection of HPV-16 E6 and E7 genes (expressing keratin 14 but not keratin 10, characteristic of basal keratinocytes) [28], was obtained from the American Type Culture Collection (ATCC) (Manassas, VA). Cells were cultured in Keratinocyte-SFM (1X) containing 5 ng/mL human recombinant EGF without bovine pituitary extract, and supplemented with 5 mL Glutamax^{TM} (all from Gibco) and 100 units/ml penicillin and 100 μg/mL streptomycin (Hyclone, Logan, UT) at 37 °C in 5% CO$_2$. As^{III} was undetectable in the medium. Visual examination of the cultured cells under a phase contrast light microscope showed cells with rounded to columnar morphology. The karyotype for the cell line is 71-86,XXY,+1,-2,+3,+5,-6,+7,+8,+9,-10,+11,-12,+13,+14,+16,add(17)(p11.2),+18,+19,+20,+20,+2-9mar[cp20]. Cytogenetic analysis revealed the presence of an abnormal hyper-triploid clone characterized by loss of chromosomes 2, 6, 10, and 12; gain of chromosomes 1, 3, 5, 7, 8, 9, 11, 13, 14, 16, 18, 19, 20, and several marker chromosomes; and additional material of unknown origin on the short arm of chromosome 17. The cp abbreviation denotes that the karyotype is a composite, due to karyotypic heterogeneity and chromosome complexity and morphology within the cells analyzed. Cells used for the study were passage 3 through passage 9.

2.3. Determination of cell viability

Ninety-six well plates were seeded with approximately 6000 cells/well. Each plate contained eight control wells (C = 0 μM As^{III} + growth medium), eight wells at each of the eight lowest concentrations (0.25 μM ≤ C_i ≤ 7 μM), four wells at each remaining concentration (C_i ≥ 10 μM), and four wells containing growth medium but no cells for use as assay blanks. Twenty-four hours after seeding, treatment with As^{III} at the concentrations listed above was begun and continued for 72 h, a treatment period selected based on previous similar studies including from our own laboratory showing that period to be adequate to reliably elicit an approximate maximal magnitude of measured cytotoxicity using the MTT assay [13,26]. At the end of the treatment period, cell viability was determined by the MTT assay [29]. Absorbance (optical density, S) of each well was determined at 570 nm using a microplate reader (Bio-Tek Elx800, Winooski, VT). Estimated viability (S_i) in the ith concentration group of treated cells on each plate was re-expressed as a corresponding percentage viability (PS$_i$ = 100% S_i/S_o); in other words as a ratio of exposed cell viability (S_i) relative to the control (unexposed) cell viability (S_o) measured on that plate. A total of 54 plates from eight experiments conducted over a 4-month period were analyzed in this way (Table 1). Preliminary experiments using unexposed and exposed HEK001 cells cultured as described demonstrated no significant effect of plate-specific well position on measured viability (data not shown).

2.4. Data analysis

The value and variance of PS$_i$ were estimated as E(PS$_i$) ~100%{[E(S)/E(S$_o$)] (1+γ_0^2)} (reflecting a 1st-order correction for ratio-estimation bias) and Var(PS$_i$) ~[E(S$_i$)/E(S$_o$)]^2 (γ_i^2 + γ_0^2), respectively, where γX = SD(X)/E(X) = the coefficient of X-variation for X = S_i or S_o, and E(X), Var(X), and SD(X) = [Var(X)]$^{1/2}$ denote the expected value, variance, and standard deviation of X, respectively [30]. Because preliminary data analyses indicated substantial, unanticipated variability in observed patterns of viability dose-response, viability data for each plate were analyzed in two stages. First, plate viability data were fit as a function of As^{III} concentration C to the following generalized lognormal cell-viability model (LNS)

$$F(C) = (PS/100\%) = P_o + P\exp(-bC)$$
$$+ (1-P)\Phi(\ln(C/GM)/\ln(GSD)) \qquad (1)$$

Table 1
LNS model fits to plate-specific viability data and related statistics.[a,c]

Plate (j)	N_x	N_p	i_j	P	P_o	b (%/μM)	GM (μM)	GSD	R^2	$p_{fit,adj}$
1	1	14	7	0.027	0.094	89.2	18.3	1.15	0.958	0.995
2	1	14	1	0	0	118.	17.9	1.53	0.950	0.995
3	1	14	2	0.095	0.085	7.46	19.5	1.24	0.972	0.995
4	1	14	2	0.101	0.092	8.76	19.8	1.28	0.976	0.995
5	2	16	1	0	0	113.	17.2	1.53	0.881	0.995
6	2	16	4	0.019	0.051	93.4	16.6	1.28	0.968	0.995
7	2	16	1	0	0.095	102.	21.4	1.20	0.867	0.995
8	2	16	1	0	0.056	61.7	18.8	1.33	0.791	0.995
9	2	16	1	0	0.070	101.	16.2	1.34	0.891	0.995
10	3	18	3	0.106	0.024	85.8	13.4	1.40	0.983	0.995
11	3	18	1	0.034	0.021	74.3	11.2	1.45	0.970	0.995
12	3	18	1	0.142	0.015	98.7	12.6	1.47	0.975	$<10^{-7}$
13	4	18	2	0.277	0.050	8.93	15.1	1.46	0.937	~0
14	4	18	4	0.359	0.045	4.26	15.9	1.34	0.965	0.995
15	4	18	9	0.418	0	0.419	17.6	1.53	0.940	0.061
16	4	18	3	0.284	0	4.54	17.5	1.50	0.931	0.665
17	4	18	4	0.250	0.028	3.14	14.9	1.58	0.959	0.995
18	4	18	6	0.330	0.058	1.44	17.4	1.27	0.935	0.684
19	5	19	2	0.192	0	8.54	13.6	1.53	0.963	0.995
20	5	19	2	0.200	0.023	7.95	12.8	1.53	0.940	0.435
21	5	19	1	0.105	0.035	108.	13.0	1.40	0.951	$<10^{-4}$
22	5	19	3	0.214	0.032	7.53	16.1	1.29	0.829	$<10^{-4}$
23	5	19	2	0.215	0.026	9.06	14.2	1.39	0.909	10^{-8}
24	5	19	2	0.225	0.024	9.73	14.6	1.45	0.853	0.995
25	6	6	3	0.103	0.041	104.	14.5	1.43	0.953	10^{-5}
26	6	6	3	0.162	0.092	4.85	18.5	1.46	0.907	0.995
27	6	6	1	0.011	0	106.	18.0	1.42	0.904	0.995
28	6	6	3	0.085	0.085	5.51	17.7	1.37	0.914	0.995
29	6	6	2	0.179	0	8.55	17.8	1.46	0.957	0.995
30	6	6	7	0.293	0.119	9.69	19.9	1.04	0.793	0.115
31	7	8	4	0.275	0.013	3.28	20.7	1.52	0.851	0.995
32	7	8	8	0.318	0.114	0.883	22.2	1.12	0.953	0.995
33	7	8	2	0.269	0.056	16.7	20.1	1.35	0.926	0.995
34	7	8	2	0.258	0	8.79	15.1	1.72	0.818	0.995
35	7	8	9	0.209	0	0.434	22.6	1.44	0.895	0.995
36	7	8	10	0.291	0.123	0.416	23.5	1.01	0.949	0.995
37	7	8	4	0.269	0	101.	22.1	1.42	0.807	0.995
38	7	8	2	0.372	0	17.1	18.8	1.47	0.849	0.995
39	7	8	2	0.067	0.113	8.45	13.7	1.77	0.933	0.995
40	7	8	3	0.317	0.085	5.84	21.5	1.17	0.790	0.995
41	7	8	1	0	0	99.8	17.4	1.69	0.827	0.995
42	7	8	1	0.037	0	8.97	16.5	1.85	0.847	0.995
43	8	9	2	0.174	0	13.0	21.7	1.47	0.880	0.995
44	8	9	2	0.165	0	7.36	17.6	1.56	0.946	0.995
45	8	9	3	0.135	0.160	4.72	20.6	1.21	0.909	0.995
46	8	9	5	0.291	0	1.55	19.8	1.53	0.966	0.995
47	8	9	2	0.107	0.126	7.43	20.8	1.22	0.937	0.995
48	8	9	1	0.215	0.073	18.21	19.6	1.35	0.929	0.995
49	8	9	1	0.239	0.092	16.7	19.6	1.37	0.946	0.995
50	8	9	7	0.178	0.117	18.8	20.4	1.27	0.966	0.995
51	8	9	7	0.261	0.112	28.7	21.2	1.13	0.896	0.995
52	8	9	4	0.142	0	83.7	20.5	1.54	0.949	0.995
53	8	9	3	0.207	0.123	7.76	20.7	1.17	0.941	0.995
54	8	9	3	0.079	0.040	43.0	18.8	1.43	0.963	0.995
AM[a]	All	–	–	0.172	0.0483	35.0	17.9	1.40	0.915	0.829
SD[a]	All	–	–	0.113	0.0462	41.4	2.97	0.173	0.0546	0.353
SEM[a]	All	–	–	0.015	0.0063	5.64	0.404	0.0236	0.0074	0.048
AM[a,b]	–[b]	–	–	0.151	0.0511	35.1	16.9	1.41	0.952	0.821
SD[a,b]	–[b]	–	–	0.091	0.0419	41.2	2.94	0.138	0.0172	0.362
SEM[a,b]	–[b]	–	–	0.017	0.0079	7.76	0.555	0.0261	0.0033	0.068

[a] LNS model variables (see Methods); those labeled without units are unitless; rational-valued entries listed are shown rounded to three significant digits. N_x = experiment #; N_p = # cell-culture passages for cells used in this experiment; i_j = initial index of concentrations C_i ($1 \le i_j \le 13$) modeled for experiment j when data were subsequently combined over multiple experiments using Eq. (2) (see Methods, Results); R^2 = squared coefficient of correlation (fraction of variance explained by regression); $p_{fit,adj}$ = p-value of chi-square goodness of fit test adjusted for $n = 54$ independent tests (values $\le 10^{-10}$ are listed as ~0); AM = arithmetic mean; SD = standard deviation; SEM = standard error of the mean; – = not applicable.

[b] Summary statistics for the subset of 28 "best-fit" plates (Plates 1, 2, 3, 4, 6, 10, 11, 12, 13, 14, 16, 17, 19, 20, 21, 25, 28, 29, 33, 39, 44, 47, 48, 49, 50, 52, 53, and 54) for which $R^2 \ge 0.91$ and B ≥ 2 (see Methods).

[c] Cell viability in a total of 4965 [=54(8×9 + 4×5) − 3] well measures were obtained in this study, excluding three defective measures involving C_i on plate j, specifically for: $\{i,j\} = \{1,30\}$, $\{5,16\}$, and $\{8,15\}$. For the "best-fit" subset of 28 plates, the corresponding total number of well measures is 2351.

In this model, P_o is the fraction of HEK001 cells that appeared to be relatively resistant (RR) to As^{III}-induced viability reduction in each assay conducted, P is the assumed fraction of cells appeared to be relatively highly susceptible or hypersusceptible (HS) to As^{III}-induced viability reduction, and b is a rate constant governing assumed 1st-order loss of HS cells exposed to As^{III}. In Eq. (1), ln denotes the natural logarithm, $\Phi(z)$ denotes the cumulative standard normal distribution function evaluated at argument z, and z

here involves functions of the geometric mean (GM) and geometric standard deviation (GSD) governing assumed lognormal loss of the remaining fraction, $1- P_o -P$, of As^{III}-exposed cells. This remaining fraction represents those HEK001 cells in each assay that appeared to exhibit an intermediate or typical-sensitivity (TS) response to As^{III} cytotoxicity—the level of sensitivity that was observed to pertain to most of the HEK001 cells examined in each assay. Eq. (1) implies that as C increases, $F(C)$ increases from $F(0) = P_o$ to a limiting value of $F(\infty) = 1-P$.

In stage 1, the LNS model was fit to plate-specific estimates of C_i-specific viability (PS_i) by nonlinear weighted least-squares regression (NLWLSR), using inverse variances estimated as described above as weights [31,32], and corresponding regression-explained fraction of total plate-specific PS_i variance (R^2) and chi-square goodness of fit statistics were also calculated.

In stage 2, data were combined over all plates and modeled as follows to characterize the dose-response relationship for As^{III} cytotoxicity specifically in TS cells defined above. Estimated PS_i values for each plate j were adjusted as follows

$$PS_{i,j}^{adj} = (PS_i - 100\%P_o)/(1 - P_o - P), i = i_j, ...13, j = 1, ..., 54 \quad (2)$$

to reflect conditioning on LNS-model parameter values of $P_o = P = 0$—that is, to represent a purely lognormal (LN) model of viability of TS cells. The initial concentration index $i_j \geq 1$ used for each jth plate was calculated as Min(i) over indices $i \in \{1,...,13\}$ conditional on

$$C_i \geq F_{LNS}^{-1}(100.5\{1-P\}) \quad (3)$$

where F_{LNS} is the LNS model (Eq. (1)) fit to PS_i estimates obtained for plate j, and $F_{LNS}^{-1}(p)$ denotes the concentration predicted by this model at viability-response level $PS = 100p\%$ ($0 \leq p \leq 1$). Condition 3 thus excludes from $PS_{i,j}^{adj}$ all those points in PS_i for plate j at which the response predicted by the LNS model for this plate is likely to be due only to HS cells. Eq. (2) and Condition 3 thus jointly imply that models fit to each jth set of $PS_{i,j}^{adj}$ data characterize a response that pertains only to TS cells, and not to either HS or RR cells.

Mean values of combined plate-specific $PS_{i,j}^{adj}$ data at each concentration C_i, weighted by the inverse-square of its respective standard error of the mean (SEM), were then fit numerically by NLWLSR as described above to LN, Cubic (C), Linear-Cubic (LC), and Hormetic-Cubic (HC) dose-response models defined by Eqs. (4)–(7), respectively:

$$PS_{LN}(C) = 100\%\{F_{LNS}(C)|(P_o = P = 0)\} \quad (4)$$

$$PS_C(C) = 100\%\{\exp(-bC^3)\} \quad (5)$$

$$PS_{LC}(C) = 100\%\{\exp(aC - bC^3)\} \quad (6)$$

$$PS_{HN}(C) = \{30/d\}[\exp(-aC) - \exp(-\{a+d\}C)] + 100\%\{\exp(-bC^3)\} \quad (7)$$

These fits were obtained for the entire set of 54 plates examined, and for a subset of (28) of "best-fit" plates for each of which a relatively predictive fit was obtained ($R^2 \geq 0.91$), together with an estimate of the LNS initial-slope parameter b that was not relatively small ($b \geq 2$). The latter condition served to reduce ambiguity concerning the estimated LNS parameter P during stage 2 of data analysis.

Assessments of PS and $PS_{i,j}^{adj}$ data normality were done by Shapiro-Wilk tests [33], corresponding variance homogeneity was assessed by Bartlett's tests [34], and p-value adjustments to corresponding p_{adj} values that account for multiple independent tests performed were done by Hommel's modified Bonferroni procedure [35]. Nested F-tests, yielding statistics $F_{df,df2}$ with df1 and df2° of freedom, were used to assess the significance of improved fits by $PS_{LC}(C)$ and by $PS_{HN}(C)$ each compared to $PS_C(C)$ [36]. To compare means of $PS_{i,j}^{adj}$ data, parametric one-way analysis of variance or (where indicated in case of unequal variances) nonparametric Kruskal-Wallis (KW) tests were used [34,37]. All calculations were performed using *Mathematica* 10.2® [32].

3. Results

MTT measures obtained for 216 blank wells had an average (± 1 SD) value of 0.000037 (± 0.0014). The eight batches of plate-specific control measures (S_o) were each approximately normally distributed with means of 0.592–0.842 and had unequal variances ($p < 10^{-7}$, by Shapiro-Wilk test); the batch-specific means differed significantly ($p < 10^{-7}$, by Kruskal-Wallis test). The combined 54 sets of plate-specific sets of S_o measures obtained had an average (± 1 SD) value of 0.731 (± 0.107), each of these sets was approximately normally distributed ($p_{adj} > 0.13$), and all sets combined had significantly unequal variances ($p = 0.000052$) and means ($p = \sim 0$, by KW test). The latter observation justified characterizing viability data on a plate-specific basis. Summaries of unadjusted viability (PS) data and corresponding LNS-model fit statistics obtained for

Table 2
Summary of adjusted viability data ($PS_{i,j}^{adj}$).[a]

i	C_i (µM)	All plates (n = 54)[b]				Plates with $R^2 \geq 0.91$ and $b \geq 2$ (n = 28)[b]			
		Mean (%)	SEM (%)	N_j	p_{adj}	Mean (%)	SEM (%)	N_j	p_{adj}
1	0.25	107.2	1.85	13	0.935	108.7	1.92	6	0.910
2	0.50	108.2	2.29	28	0.930	108.6	1.47	16	0.910
3	1	104.2	1.61	38	0.376	104.4	1.67	22	0.061
4	2	107.4	1.69	44	0.935	105.8	1.72	26	0.910
5	3	101.7	1.74	45	0.935	99.6	1.62	26	0.910
6	4	103.1	1.65	46	0.890	100.7	1.41	26	0.910
7	5	96.4	1.44	50	0.935	97.2	1.28	28	0.910
8	7	94.5	1.46	51	0.041	92.7	1.56	28	0.027
9	10	88.9	1.82	53	0.935	86.2	1.99	28	0.910
10	15	55.2	2.66	54	0.935	63.4	3.67	28	0.051
11	20	36.6	2.54	54	0.935	28.3	3.06	28	0.910
12	25	5.21	1.50	54	0.547	3.50	1.63	28	0.910
13	30	3.40	0.79	54	0.001	3.47	0.79	28	0.062

[a] Mean = weighted arithmetic mean of adjusted percent-viability data using inverse estimated variances as weights; $C_i = i^{th}$ test concentration of As^{III}; SEM = standard error of the mean; N_j = # plates from which data at concentration C_i were averaged (only concentrations $i = i_j$ through $i = 13$ were included from each jth plate—see Methods and Table 1); p_{adj} = p-value of Shapiro-Wilk test of approximate normality of estimated weighted means, adjusted for 13 independent tests. Mean values are shown to $\geq 0.1\%$ accuracy or 3 significant digits, and SEM values to $\geq 0.01\%$ accuracy.
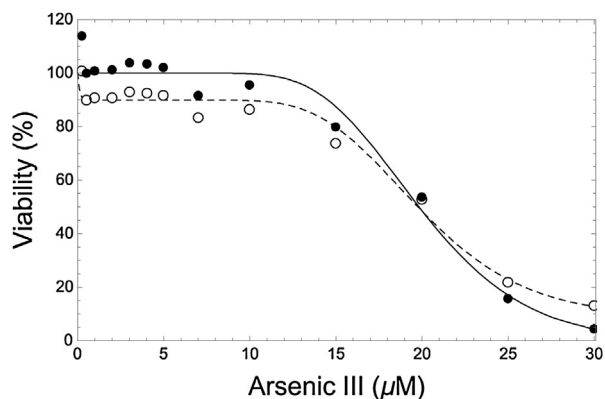[b] See Table 1.

Fig. 1. Observed viability data (open points) and corresponding LNS-model fit (dashed curve) for plate #4, compared to data values (solid points) that are all adjusted to reflect this fitted model with assumed parameter values of $P = P_o = 0$ (solid curve).

each plate are listed in Table 1, based on MTT cell-viability measures obtained for nearly 5000 control and treated wells (see Table 1, note c). Of the 54 LNS-model fits summarized in Table 1, only four are clearly inconsistent ($p_{fit,adj} \leq 0.01$) with the modeled data conditional on the estimated errors in estimated mean response, but all fits nevertheless predict those mean-response patterns reasonably well ($0.790 \leq R^2 \leq 0.983$). Six of the variables (N_p, P, P_o, B, R^2, $p_{fit,adj}$) defined in Table 1 exhibited no significant Pearson product-moment correlations ($p_{adj} > 0.20$), except for a negative association between estimates for LNS model parameters b and P ($r = -0.66$, $p_{adj} = 10^{-7}$). A similar correlation pattern and similar summary statistics for estimated parameters and LNS-model fits were obtained for a subset of 28 "best-fit" plates (Table 1). Individual LNS-model fits to these 28 data sets appear in Supplemental Materials.

Adjusted viability data (defined by Eq. (2)) that were combined for dose-response analysis are summarized in Table 2. Fits of LN, Cubic, LC, and HC models obtained to the complete set of adjusted data, and to the "best-fit" data subset, are shown in Figs. 1 and 2, respectively. Corresponding fit details and statistics are listed in Table 3. Using data from all $n = 54$ plates as well as only from the 28 "best-fit" plates, approximately equal levels of adjusted mean viability ($p > 0.30$) occurred at the five concentrations $\leq 3\,\mu M$ As^{III} examined. When combined (using either $n = 54$ or $n = 28$ plates), the overall mean level of relative viability at concentrations $\leq 3\,\mu M$ As^{III} significantly exceeded that exhibited by unexposed (control) cells ($p \leq 10^{-6}$). Although the LN, Cubic, LC, and HC models were each very predictive ($R^2 > 0.97$), none were statistically consistent with the entire corresponding data set examined ($p < 10^{-5}$). The LC model fit to each data set contained a linear coefficient that is positive (*i.e.*, hormetic, which in the present context, indicates increased viability with increasing concentration at low concentrations), but not significantly so (Table 3). LC model fits were not significantly better than corresponding Cubic-model fits ($F_{12,11} = 0.53$ and $p = 0.85$ with $n = 54$, $F_{12,11} = 0.18$ and $p = 0.997$ with $n = 28$). The HC model, which also exhibits low-dose hormetic behavior, provided the best fit to the combined data ($R^2 = 0.995$) (Table 3), and provided a significantly better fit than the Cubic model ($F_{12,10} = 5.62$ and $p = 0.0051$ with $n = 54$, $F_{12,10} = 30.14$ and $p = 0.00081$ with $n = 28$).

4. Discussion and conclusions

The current study used a greater number of replicate plates than in any previously reported study of *in vitro* As^{III} cytotoxicity and assessed cytotoxicity at many different concentrations.
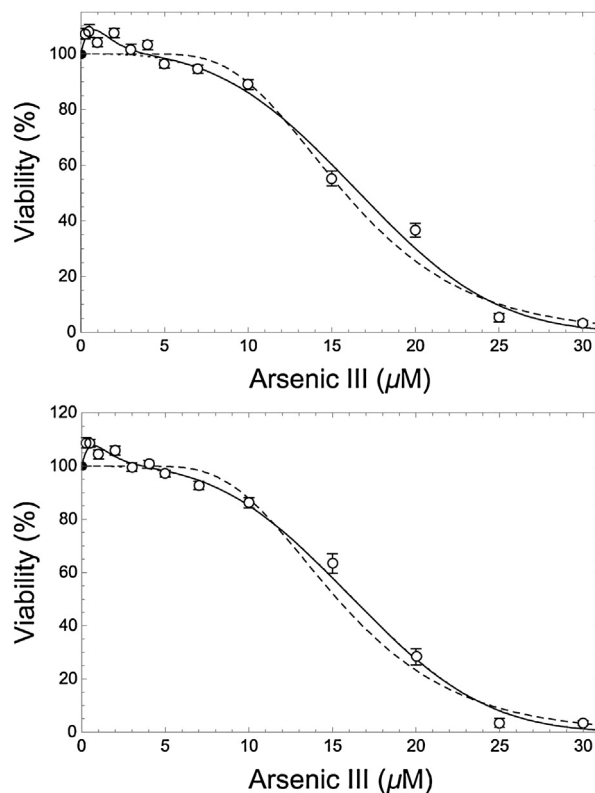

Fig. 2. Model fits to adjusted viability data from all 54 plates (top plot), and from 28 plates for which the LNS model yielded fits (to corresponding unadjusted data sets) that are all relatively predictive ($R^2 \geq 0.91$) and have relatively steep initial slopes ($b \geq 2$—see Table 1) (bottom plot). Error bars denote ± 1 SEM. Fitted models shown in each plot are: lognormal (dashed curve), cubic-hormetic (solid curve), and cubic (dotted curve, which nearly coincides with the dashed and solid curve at $C \leq 3\,\mu M$ and $C \geq 4\,\mu M$, respectively).

Markedly variable and unexplained dose-response patterns were observed concerning unadjusted data on HEK001 cell viability after As^{III} exposure, The LNS model plausibly describes diverse dose-response patterns of As^{III} cytotoxicity observed for an estimated fraction $1 - P - P_o$ of HEK001 cells in each test that appeared to exhibit a typical level of resistance to As^{III} cytotoxicity. Each test-specific fraction P_o of apparently highly resistant cells was estimated after adjusting each corresponding set of viability data to exclude an estimated proportion P of tested cells that appeared to be relatively highly susceptible to cytotoxicity induced at very low As^{III} concentrations (as low as $0.25\,\mu M$). Such unexpected and unexplained phenotypic heterogeneity in apparent ultra-low-dose sensitivity to As^{III} was characterized as inter-test variation in the fraction P, estimated to range from 0 to 42%, and to average approximately 17% (Table 1). This heterogeneity challenges the hypothesis that As^{III} cytotoxic effects have a dose-response threshold (*i.e.*, do not occur at relatively low doses), to the extent that the fractions of evidently highly As^{III}-susceptible HEK001 cells that were estimated to occur in this study accurately model hypersensitive cell phenotypes that also occur *in vivo*. Only if such relatively highly susceptible subpopulations of cultured HEK001 cells are not relevant *in vivo*—for example, if they are an unrealistic artifact of this line of cultured cells, or of the *in vitro* cell culture conditions used—would the good fits obtained in this study by the LNS model to adjusted HEK001 cell-viability data provide evidence consistent with a threshold-like dose-response for As^{III} cytotoxicity, conditional on the assumption that $P = 0$ under biologically relevant conditions *in vivo*. In contrast, patterns of As^{III}-induced cell toxicity observed in this study indicate that As^{III} is cytotoxic to a relatively small and relatively highly

Table 3
Model fits to adjusted viability data ($PS_{i,j}^{adj}$).[a]

Model	Plates included[b]	Parameter	Estimate	SE	$p_{=0}$	R^2	p_{fit}
LN	54	GM	15.77	0.705	$<10^{-9}$	0.979	~0
		GSD	1.435	0.061	~0		
LN	28	GM	15.30	0.860	$<10^{-8}$	0.977	~0
		GSD	1.442	0.070	~0		
Cubic	54	$b\,(\times10^4)$	1.500	0.154	$<10^{-8}$	0.983	~0
	28	$b\,(\times10^4)$	1.612	0.208	$<10^{-5}$	0.986	~0
LC	54	$a\,(\times10^3)$	2.889	3.93	0.48	0.983	~0
		$b\,(\times10^4)$	1.603	0.218	10^{-5}		
	28	$a\,(\times10^3)$	1.695	4.20	0.69	0.986	~0
		$b\,(\times10^4)$	1.681	0.280	$<10^{-4}$		
HC	54	a	1.207	8.99	0.90	0.992	$<10^{-5}$
		d	0.1678	18.9	0.99		
		$b\,(\times10^4)$	1.502	0.116	10^{-7}		
	28	a	1.053	1.69	0.55	0.995	0.0008
		d	0.7963	4.24	0.19		
		$b\,(\times10^4)$	1.681	0.116	$<10^{-6}$		

[a] Models LN, Cubic, LC, and HC are defined by Equations 4–7, respectively (Methods). those labeled without units are unitless. SE = standard error; p_0 = p-value from a *t*-test of the null hypotheses that the parameter value is zero (values $\leq10^{-10}$ are listed as ~0); R^2 = squared coefficient of correlation (fraction of variance explained by regression); p_{fit} = p-value of chi-square goodness of fit test. Parameter and SE estimates are rounded to 4 and at least 3 significant digits, respectively.
[b] See Table 2.

sensitive subset of HEK001 cells in approximate linear proportion to the As^{III} concentration (consistent with slope parameter *b* in Eq. (1)). To the extent that "typical-sensitivity" HEK001 cells posited by the LNS model do exist, data obtained in this study do not provide evidence that low concentrations of As^{III} are toxic to these cells in linear proportion to As^{III} concentration. Consequently, results obtained in this study are novel and interesting, and merit further study to address the question of whether and to what extent sub-populations of cells that are relatively highly sensitive to As^{III} (in contrast to cells that exhibit more typical levels of sensitivity to As^{III}) exist in other cell lines and *in vivo*.

One possible explanation for the substantial variability in esti-mated values of *P* obtained in this study is that variation in values of *P*, as well as our observation of statistically significantly increased adjusted viability in the (presumptive) remainder of "typical-sensitivity" cells exposed to ≤3 vs. 0 μM As^{III}, was due to karyotypic heterogeneity present in the cell line. The cell line was derived originally from cells from the scalp of a 65-year-old male [28] that were transfected with a plasmid p1321 containing human papillo-mavirus (HPV) 16 E6 and E7 genes, which may have resulted in the heterogeneity of the karyotype. Alternatively, the observed hetero-geneity might be a result of cell passages, or possibly to artifacts of variable aspects of *in vitro* testing such as plating-induced damage to a fraction (*P*) of plated HEK001 cells. Additional experiments will be required to determine the cause of substantial variation in the apparent value of *P* that was observed in this study.

Ideally, a detailed study of this type would be repeated using multiple cell lines and multiple viability and viability assay meth-ods in parallel, despite the fact that low-concentration As^{III}-induced cytotoxicity is well known to involve induction of apoptotic path-ways [38–42]. Even using a single cell line and a single assay method for reasons of practical feasibility for a first study conducted at this level of detail, the study design was quite expensive and very labor intensive. Nevertheless, results from this study represent a monumental effort that clearly yielded interesting and unexpected results. Future studies can extend this approach to additional cell lines and assay methods.

Acknowledgements

Appendix A. Supplementary data

Supplementary data associated with this article can be found, in the online version, at http://dx.doi.org/10.1016/j.toxrep.2016.12.003.

References

[1] IARC, IARC monographs on the evaluation of carcinogenic risks to humans, in: Some Drinking-Water Disinfectants and Contaminants, Including Arsenic, International Agency for Research on Cancer (IARC), World Health Organization, France, 2004.

[2] J.M. Chiou, S.-L. Wang, C.-J. Chen, C.-R.W. Deng Lin, T.-Y. Tai, Arsenic ingestion and increased microvascular disease risk: observations from the south-western arseniasis-endemic area in Taiwan, Int. J. Epidemiol. 343 (2005) 936–943.

[3] E.A. Maull, H. Ahsan, J. Edwards, M.P. Longnecker, A. Navas-Acien, J. Pi, E.K. Silbergeld, M. Styblo, C.-H. Tseng, D. Loomis, Evaluation of the association between arsenic and diabetes: a National Toxicology Program workshop review, Environ. Health Perspect. 120 (2012) 1658–1670.

[4] M.F. Naujokas, B. Anderson, H. Ahsan, H.V. Aposhian, J.H. Graziano, C. Thompson, W.A. Suk, The broad scope of health effects from chronic arsenic exposure: update on a worldwide public health problem, Environ. Health Perspect. 121 (2013) 295–302.

[5] C.O. Abernathy, W.R. Chappell, M.E. Meek, H. Gibb, Guo H-R. Is ingested inorganic arsenic a threshold carcinogen, Fundam. Appl. Toxicol. 29 (1996) 168–175.

[6] H. Carlson-Lynch, B.D. Beck, P.D. Boardman, Arsenic risk assessment, Environ. Health Perspect. 102 (4) (1994) 354–355.

[7] H.J. Clewell, P.R. Gentry, H.A. Barton, A.M. Shipp, J.W. Yager, M.E. Andersen, Requirements for a biologically realistic cancer risk assessment for inorganic arsenic, Int. J. Toxicol. 18 (1999) 131–147.

[8] S.M. Cohen, L.L. Arnold, B.D. Beck, A.S. Lewis, M. Eldan, Evaluation of the carcinogenicity of inorganic arsenic, Crit. Rev. Toxicol. 43 (2013) 711–752.

[9] K.A. Moon, E. Guallar, J.G. Umans, R.B. Devereux, L.G. Best, K.A. Francesconi, W. Goessler, J. Pollak, E.K. Silbergeld, B.V. Howard, A. Navas-Acien, Association between exposure to low to moderate arsenic levels and incident cardiovascular disease: a prospective cohort study, Ann. Intern. Med. 159 (2013) 649–659.

[10] K.F. Rodriguez, E.K. Ungewitter, Y. Crespo-Mejias, C. Liu, B. Nicol, G. Kissling, H. Yao, Effects of in utero exposure to arsenic during the second half of gestation on reproductive end points and metabolic parameters in female CD-1 mice, Environ. Health Perspect. 124 (2016) 336–343.

[11] P.R. Gentry, T.B. McDonald, D.E. Sullivan, A.M. Shipp, J.W. Yager, H.J. Clewell 3rd, Analysis of genomic dose-response information on arsenic to inform key events in a mode of action for carcinogenicity, Environ. Mol. Mutagen. 51 (2010) 1–14.

[12] J.W. Yager, P.R. Gentry, R.S. Thomas, L. Pluta, A. Efremenko, M. Black, L.L. Arnold, J.M. McKim, P. Wilga, G. Gill, K.Y. Choe, H.J. Clewell, Evaluation of gene expression changes in human primary uroepithelial cells following 24-hr exposures to inorganic arsenic and its methylated metabolites, Environ. Mol. Mutagen. 54 (2013) 82–98.

[13] P.R. Dodmane, L.L. Arnold, S. Kakiuchi-Kiyota, F. Qiu, X. Liu, S.I. Rennard, S.M. Cohen, Cytotoxicity and gene expression changes induced by inorganic and organic trivalent arsenicals in human cells, Toxicology 312 (2013) 18–29.

[14] S.M. Cohen, L.L. Arnold, J.E. Klaunig, J.I. Goodman, Response to the Waalkes et al., Letter to the editor concerning our "Letter to the editor, Re: lung tumors in mice induced by "whole-life" inorganic arsenic exposure at human relevant doses, Waalkes et al., Arch Toxicol, 2014, Arch. Toxicol. 89 (2015) 2167–2168.

[15] M.S. Sidhu, K.P. Desai, H.N. Lynch, L.R. Rhomberg, B.D. Beck, F.J. Venditti, Mechanisms of action for arsenic in cardiovascular toxicity and implications for risk assessment, Toxicology 331 (2015) 78–99.

[16] J.S. Tsuji, V. Perez, M.R. Garry, D.D. Alexander, Association of low-level arsenic exposure in drinking water with cardiovascular disease: a systematic review and risk assessment, Toxicology 323 (2014) 78–94.

[17] J.S. Tsuji, V. Perez, M.R. Garry, D.D. Alexander, Association of low-level arsenic exposure in drinking water with cardiovascular disease: a systematic review and risk assessment, Toxicology 323 (2014) 78–94.

[18] J.S. Tsuji, M.R. Garry, V. Perez, E.T. Chang, Low-level arsenic exposure and developmental neurotoxicity in children: a systematic review and risk assessment, Toxicology 337 (2015) 91–107.

[19] S.H. Lamm, S. Robbins, R. Chen, J. Lu, B. Goodrich, M. Feinleib, Discontinuity in the cancer slope factor as it passes from high to low exposure levels – arsenic in the BFD-endemic area, Toxicology 326 (2014) 25–35.

[20] S. Lamm, H. Ferdosi, E. Dissen, J. Li, J. Ahn, A systematic review and meta-regression analysis of lung cancer risk and inorganic arsenic in drinking water, Int. J. Environ. Res. Public Health 12 (2015) 14990.

[21] K.T. Bogen, Linear-no-threshold default assumptions for noncancer and nongenotoxic-cancer risks: a mathematical and biological critique, Risk Anal. 36 (3) (2016) 589–604 http://onlinelibrary.wiley.com/doi/10.1111/risa.12460/epdf.

[22] S.O. Simmon, C.-Y. Fan, K. Yeoman, J. Wakefield, R. Ramabhadran, NRF2 oxidative stress induced by heavy metals is cell type dependent, Curr. Chem. Genomics 5 (2011) 1–12.

[23] S.J. Shukla, R. Huang, S.O. Simmons, R.R. Tice, K.L. Witt, D. VanLeer, R. Ramabhadran, C.P. Austin, M. Xia, Profiling environmental chemicals for activity in the antioxidant response element signaling pathway using a high throughput screening approach, Environ. Health Perspect. 120 (8) (2012) 1150–1156.

[24] J. Liu, K.C. Wu, Y.F. Lu, E. Ekuase, C.D. Klaassen, Nrf2 protection against liver injury produced by various hepatotoxicants, Oxid. Med. Cell Longev. 2013 (2013) 305861, http://dx.doi.org/10.1155/2013/305861.

[25] B. Graham-Evans, P.B. Tchounwou, H.H.P. Cohly, Cytotoxicity and proliferation studies with arsenic in established human cell Lines: keratinocytes, melanocytes, dendritic cells, dermal fibroblasts, microvascular endothelial cells, monocytes and T-cells, Int. J. Mol. Sci. 4 (2003) 13–21.

[26] E.V. Komissarova, S.K. Saha, T.G. Rossman, Dead or dying: the importance of time in cytotoxicity assays using arsenite as an example, Toxicol. Appl. Pharmacol. 202 (2005) 99–107.

[27] E.V. Komissarova, T.G. Rossman, Arsenite induced poly(ADPribosyl)ation of tumor suppressor P53 in human skin keratinocytes as a possible mechanism for carcinogenesis associated with arsenic exposure, Toxicol. Appl. Pharmacol. 243 (3) (2010) 399–404.

[28] P.B. Sugerman, M. Bigby, Preliminary functional analysis of human epidermal T cells, Arch. Dermatol. Res. 292 (2000) 9–15.

[29] T. Mosmann, Rapid colorimetric assay for cellular growth and survival: application to proliferation and cytotoxicity assays, J. Immunol. Meth. 65 (1983) 55–63.

[30] M. Kendall, A. Stuart, The advanced theory of statistics Distribution Theory, vol. 247, 4th ed., MacMillan Publishing Co., NY, 1977, pp. 260.

[31] R.J. Carrol, D. Ruppert, Transformation and Weighting in Regression, Chapman and Hall, New York, NY, 1988, pp. 9–62.

[32] Wolfram Research, Wolfram Mathematica 9 Documentation Center, Wolfram Research, Inc., Champaign, IL, 2015 (www.wolfram.com, http://reference.wolfram.com/mathematica/guide/Mathematica.html).

[33] P. Royston, Approximating the Shapiro-Wilk W-test for non-normality, Stat. Comput. 2 (3) (1992) 117–119.

[34] G.W. Snedecor, W.G. Cochran, Statistical Methods, 8th ed., Iowa State University Press, Ames, IA, 1989, pp. 217–236.

[35] S.P. Wright, Adjusted p-values for simultaneous inference, Biometrics 48 (1992) 1005–1013.

[36] S. Selvin, Practical Biostatistical Methods, Duxbury Press, Wadsworth Publishing Co., Belmont, CA, 1995, pp. 1–137.

[37] E.L. Lehman, H.J.M. D'Abrera, Nonparametrics: Statistical Methods Based on Ranks, Holden-Day, San Francisco, CA, 1975, pp. 204–210.

[38] C.G. Yedjou, P. Moore, P.B. Tchounwou, Dose- and time-dependent response of human leukemia (HL-60) cells to arsenic trioxide treatment, Int. J. Environ. Res. Public Health 3 (2) (2006) 136–140.

[39] H. Li, J. He, P. Ju, X. Zhong, J. Liu, Studies on the mechanism of arsenic trioxide-induced apoptosis in HepG2 human hepatocellular carcinoma cells, Chin. J. Clin. Oncol. 5 (2008) 22–25, http://dx.doi.org/10.1007/s11805-008-0022-6.

[40] J.J. Stevens, B. Graham-Evans, A.M. Walker, B. Armstead, P.B. Tchounwou, Cytotoxic effect of arsenic trioxide in adenocarcinoma colorectal cancer (HT-29) cells, Met. Ions Biol. Med. 10 (2008) 458–462.

[41] Y. Wang, Y. Xu, H. Wang, P. Xue, X. Li, B. Li, Q. Zheng, G. Sun, Arsenic induces mitochondria-dependent apoptosis by reactive oxygen species generation rather than glutathione depletion in Chang human hepatocytes, Arch. Toxicol. 83 (10) (2009) 899–908, http://dx.doi.org/10.1007/s00204-009-0451-x.

[42] S. Kumar, C.G. Yedjou, P.B. Tchounwou, Arsenic trioxide induces oxidative stress, DNA damage, and mitochondrial pathway of apoptosis in human leukemia (HL-60) cells, J. Clin. Exp. Cancer Res. 33 (2014) 42, http://dx.doi.org/10.1186/1756-9966-33-42.